

SCIENTIFIC REPORTS



OPEN

Evaluation of pre-analytical factors affecting plasma DNA analysis

Havell Markus¹, Tania Contente-Cuomo¹, Maria Farooq¹, Winnie S. Liang^{1,2}, Mitesh J. Borad³, Shivan Sivakumar⁴, Simon Gollins⁵, Nhan L. Tran^{1,6}, Harshil D. Dhruv¹, Michael E. Berens¹, Alan Bryce³, Aleksandar Sekulic^{1,3}, Antoni Ribas⁷, Jeffrey M. Trent^{1,2}, Patricia M. LoRusso⁸ & Muhammed Murtaza^{1,3}

Received: 3 May 2017

Accepted: 30 April 2018

Published online: 09 May 2018

Pre-analytical factors can significantly affect circulating cell-free DNA (cfDNA) analysis. However, there are few robust methods to rapidly assess sample quality and the impact of pre-analytical processing. To address this gap and to evaluate effects of DNA extraction methods and blood collection tubes on cfDNA yield and fragment size, we developed a multiplexed droplet digital PCR (ddPCR) assay with 5 short and 4 long amplicons targeting single copy genomic loci. Using this assay, we compared 7 cfDNA extraction kits and found cfDNA yield and fragment size vary significantly. We also compared 3 blood collection protocols using plasma samples from 23 healthy volunteers (EDTA tubes processed within 1 hour and Cell-free DNA Blood Collection Tubes processed within 24 and 72 hours) and found no significant differences in cfDNA yield, fragment size and background noise between these protocols. In 219 clinical samples, cfDNA fragments were shorter in plasma samples processed immediately after venipuncture compared to archived samples, suggesting contribution of background DNA by lysed peripheral blood cells. In summary, we have described a multiplexed ddPCR assay to assess quality of cfDNA samples prior to downstream molecular analyses and we have evaluated potential sources of pre-analytical variation in cfDNA studies.

Analysis of circulating cell-free DNA from plasma (cfDNA) has several potential diagnostic applications in prenatal, transplant and cancer medicine^{1–4}. In patients with cancer, a fraction of cfDNA carries tumor-specific somatic mutations. Circulating tumor DNA (ctDNA) analysis relies on detection and quantification of these mutations, against a background of cfDNA contributed by peripheral blood cells and other tissues. Total cfDNA and tumor-specific ctDNA levels in plasma vary considerably across cancer patients, cancer types and disease stages as well as during longitudinal follow-up of each patient^{5,6}. Several recent reports have described sensitive molecular methods for analysis of ctDNA^{7–9}. However, comparison between published ctDNA studies is often challenging because of differences in collection and processing of plasma samples. Our understanding of how pre-analytical factors affect performance and results of ctDNA assays is limited¹⁰.

cfDNA fragments in plasma have a modal fragment size of 160–180 bp, corresponding to DNA protected in mono-nucleosomes¹¹. One challenge when analyzing plasma DNA is the variable contribution of high molecular weight (HMW) DNA resulting from lysis of peripheral blood cells during blood processing^{12–15}. HMW DNA is not intended to be part of the molecular readout during ctDNA analysis but it can affect PCR and sequencing results. High fractions of HMW DNA in plasma can complicate PCR and tagmentation-based sequencing because these methods will incorporate intact DNA in a sample, potentially biasing the data towards wild-type alleles and increasing false negative results for somatic mutations. In contrast, ligation-based library preparation from cfDNA does not require any additional DNA fragmentation and therefore excludes intact DNA. However, if the contribution of intact DNA is not taken into account during sample quantification, library preparation can vary in performance. Ideally, rapid processing of blood samples as soon as possible after venipuncture can

¹Center for Noninvasive Diagnostics, Translational Genomics Research Institute, Phoenix, AZ, USA. ²Integrated Cancer Genomics Division & Collaborative Sequencing Center, Translational Genomics Research Institute, Phoenix, AZ, USA. ³Mayo Clinic Center for Individualized Medicine, Scottsdale, AZ, USA. ⁴Department of Oncology, University of Oxford, Oxford, United Kingdom. ⁵North Wales Cancer Treatment Centre, Rhyl, United Kingdom. ⁶Department of Cancer Biology, Mayo Clinic Arizona, Scottsdale, AZ, USA. ⁷Department of Medicine, Division of Hematology/Oncology, University of California Los Angeles Jonsson Comprehensive Cancer Center, Los Angeles, CA, USA. ⁸Department of Internal Medicine, Yale University, New Haven, CT, USA. Correspondence and requests for materials should be addressed to M.M. (email: mmurtaza@tgen.org)

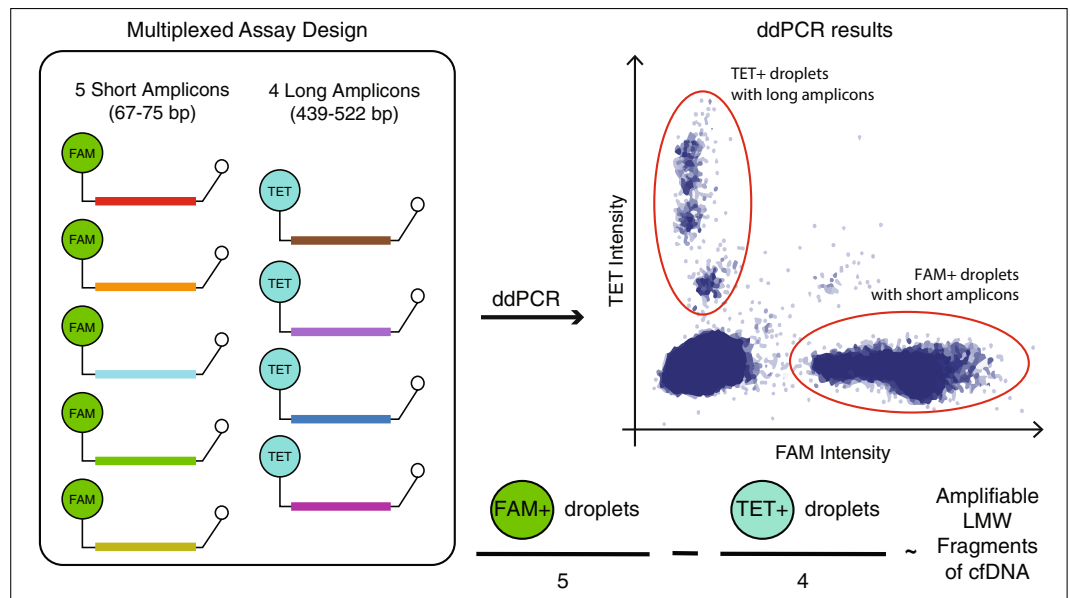


Figure 1. Schematic representation of a multiplexed droplet digital PCR approach for measuring cfDNA quantity and evaluating fragment size. We expect two populations of droplets with distinct fluorescence, each representing the sum of products from the two amplicon sets. The number of FAM-positive droplets represents 5 times the number of haploid genome equivalents (GEs) with fragments long enough to be amplified using short amplicons. Similarly, the number of TET-positive droplets represents 4 times the GEs with fragment sizes amplifiable using long amplicons. We calculate low molecular weight (LMW) cfDNA concentration as the difference between average short and long GEs. Primer sequences and amplicon sizes are listed in Supplemental Table 1 and amplicon positions relative to common SNPs are shown in Supplemental Figure 6.

overcome these issues but real-time processing of samples is challenging in clinical environments. With growing interest in cfDNA-based diagnostics, several solutions have emerged to streamline pre-analytical processing. These include special blood collection tubes that contain cell-stabilizing preservative to minimize lysis of peripheral blood cells for up to several days after venipuncture. In addition, cfDNA-focused extraction kits have been introduced that claim preferential extraction of fragmented cfDNA over HMW DNA from the same sample.

There is scarcity of robust methods that allow quality assessment of low input cfDNA samples and there are few published comparisons between pre-analytical solutions. Here, we present a multiplexed digital PCR approach that can reliably assess cfDNA quantity and contribution of HMW DNA. We use this assay to compare cfDNA extraction kits and to perform quality assessment of plasma samples across multiple archival and prospective clinical cohorts of cancer patients. We also evaluate the performance and downstream effects of blood collection tubes in matched plasma samples from healthy volunteers.

Results

Droplet Digital PCR to assess cfDNA concentration and fragment size. To enable reliable assessment of amplifiable DNA concentration and fragment size using minimal quantities of cfDNA, we designed a multiplexed ddPCR assay targeting 9 single copy genomic loci¹⁶. We included 5 short PCR amplicons with mean product size of 71 bp (range 67–75 bp) and corresponding probes labeled with FAM as well as 4 long PCR amplicons with mean product size of 471 bp (range 439–522 bp) and corresponding probes labeled with TET (Fig. 1 and Supplemental Table 1). We confirmed each individual assay amplified linearly over a range of input concentrations using quantitative PCR (qPCR; Supplemental Fig. 1). When multiplexed together on ddPCR, we expected two populations of droplets with distinct fluorescence, each representing the sum of products from the two amplicon sets. Assuming no copy number changes, the number of FAM-positive droplets represents 5 times the number of haploid genome equivalents (GEs) with fragments long enough to be amplified using short amplicons. Similarly, the number of TET-positive droplets represents 4 times the GEs with fragment sizes amplifiable using long amplicons. We calculated low molecular weight cfDNA concentration as the difference between short and long GEs. Within FAM- and TET-positive droplets, we observed distinct droplet clusters that corresponded with differences in amplicon sizes. For example, when analyzing intact DNA using this assay, we found an amplicon of 522 bp clustered at lower fluorescence levels compared to two other amplicons of 439 and 444 bp, consistent with earlier inhibition of amplification in individual droplets containing longer PCR amplicons. We used this feature to compare quantitative performance of amplicons with each other and found high correlation when analyzing intact DNA samples (Supplemental Fig. 2).

To evaluate the performance of the multiplexed assay, we analyzed control DNA with different predetermined fragment sizes (holding the DNA concentration constant across comparisons). We compared observed results with expected PCR performance, simulated using the exponential distribution, given amplicon and fragment sizes. Observed ddPCR results agreed with expected results for 150, 300, 500 and 1,000 bp fragments remarkably.

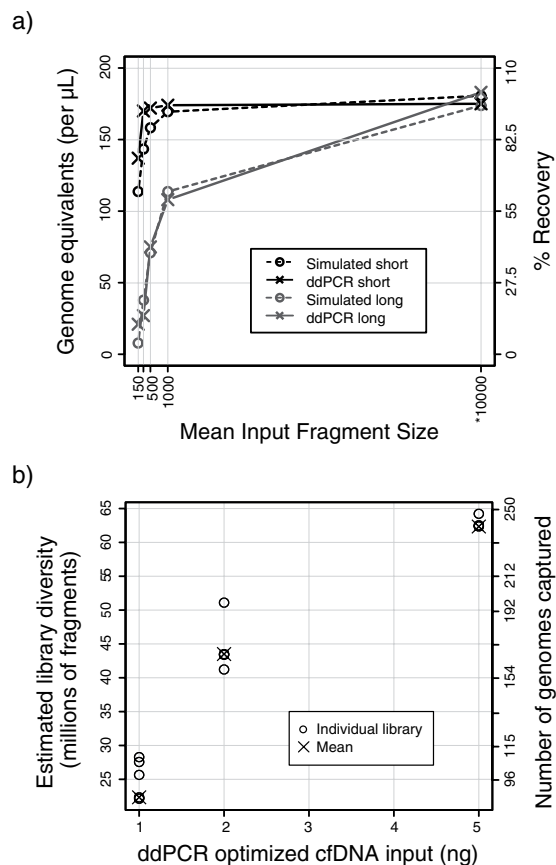


Figure 2. Evaluation of ddPCR assay performance. **(a)** Comparison of ddPCR measurements with expected results when using control DNA of known fragment size as template. Solid lines with crosses show measured ddPCR results. Dotted lines with circles show simulated data, generated using the exponential distribution with period set to fragment size. *Simulated data was generated assuming 10,000 bp fragments, a much larger period compared to the PCR amplicon sizes used here. Corresponding ddPCR measurement was performed on intact genomic DNA (without sonication). **(b)** Evaluation of sequencing library diversity obtained with cfDNA input amounts measured using the ddPCR assay. The first y-axis on the left shows projected diversity of the library in millions of unique fragments. On the second y-axis (right), library diversity has been converted into number of genome equivalents, by calculating the quotient between the projected diversity and fragments expected per haploid genome. Assuming 44 Mb exome captured region and 170 bp fragment size, we expect ~ 0.26 million fragments per haploid genome. 5, 4, and 3 individual libraries were prepared for 1, 2, and 5 ng cfDNA input respectively. These data are also listed in Supplemental Table 2.

For example, using a 71 bp amplicon and input of 150 bp DNA fragments, we expect to recover $\sim 62\%$ and we observed 75% recovery using short amplicons in our assay (Fig. 2a). We also compared ddPCR results with DNA quantification by fluorometry (Qubit) and found strong correlation (Pearson $r = 0.908$, $p = 1.18 \times 10^{-6}$, Supplemental Fig. 3). We further compared ddPCR results with DNA quantification using an electrophoretic approach (Agilent BioAnalyzer DNA High Sensitivity Assay) and found strong correlation between LMW concentrations measured using the two methods (Pearson $R: 0.809$, $p = 0.0026$, Supplemental Figure 4). To assess whether ddPCR quantification of input DNA can help overcome variability in sequencing results, we measured the concentration of low molecular weight (LMW) DNA in 5 control plasma samples to prepare and sequence 12 exome libraries made from 1, 2 and 5 ng LMW DNA. Besides input quantity, all other library preparation conditions including number of PCR cycles were similar between these replicates. Library size and diversity was estimated from 0.83–1.66 million read pairs per sample. As expected, library diversity correlated strongly with input DNA quantities (Pearson $r = 0.938$, $p = 2.48 \times 10^{-7}$; Fig. 2b and Supplemental Table 2).

Comparison of cfDNA extraction kits. To compare performance of cfDNA extraction kits and minimize the contribution of biological variation, we obtained a pooled control plasma sample. We compared 7 different extraction kits marketed for cfDNA extraction including 3 spin column-based methods and 4 magnetic beads-based methods (labeled A-G, see Supplemental Table 3). For each kit, we performed 10 replicates of DNA extraction from 1 mL plasma and quantified cfDNA yield and fragment size using ddPCR. We found wide variability in yield and fragment size across these kits (ANOVA $p = 5.01 \times 10^{-11}$ and $p = 1.16 \times 10^{-11}$ respectively, Fig. 3 and Supplemental Table 4). Highest median yield of LMW cfDNA was obtained using Kit A that uses spin

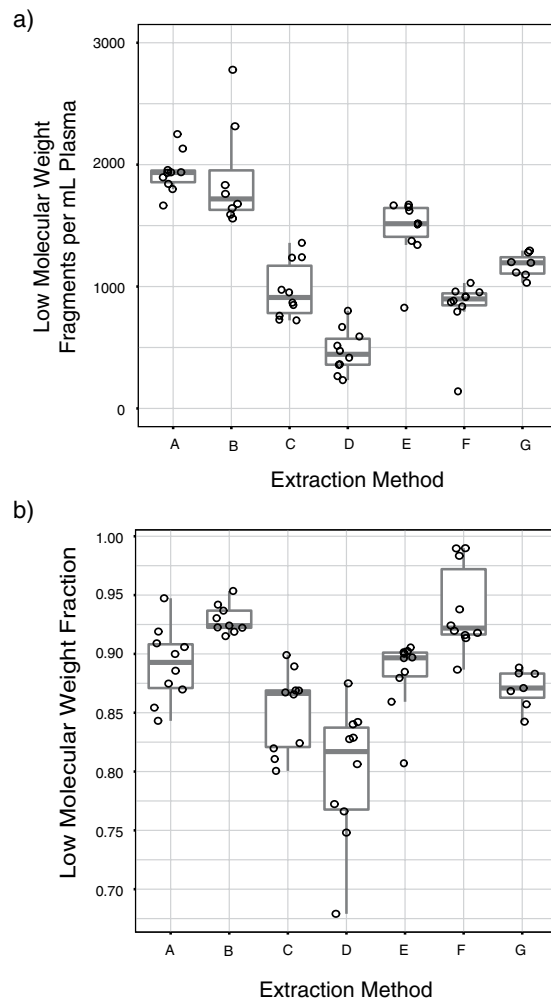


Figure 3. Evaluation of cfDNA extraction methods using ddPCR. Kits labeled A-C use spin columns and kits labeled D-G use magnetic beads for cfDNA isolation. For each extraction kit, $n = 10$ individual extractions were performed successfully, starting with 1 mL plasma volume except for kit B ($n = 9$) and kit G ($n = 7$). Aliquots from a single pool of 250 mL commercially obtained control plasma sample were used for these experiments. **(a)** Comparison of cfDNA yield (in LMW fragments/mL of plasma) across 7 extraction kits. An outlier at 5,306 LMW fragments/mL for Kit B is not shown to enhance scaling. Concentration of LMW fragments in DNA samples was calculated as the difference between average short and long GEs (as shown in Fig. 1). To calculate concentration in input plasma samples, the LMW fragment concentration in DNA samples was multiplied by elution volume and divided by input volume of plasma used during DNA extraction (1 mL). **(b)** Comparison of LMW fraction across 7 extraction kits. LMW fraction was calculated as LMW fragment concentration (difference between average short and long GEs) as a fraction of average short GEs. These data are also listed in Supplemental Table 4.

columns for cfDNA extraction (1,936 GEs/mL of plasma, $n = 10$). Median LMW fraction for Kit A was 89%. The median yield of LMW DNA using Kit B was not significantly different than Kit A but the results were more variable (1,760 LMW copies/mL plasma, t -test $p = 0.427$). Amongst methods based on magnetic beads, Kit E showed the highest yield of LMW DNA (median 1,515 LMW copies/mL, $n = 10$) and a LMW fraction comparable to Kit A (median 90%). In comparison to Kit A, the yield was significantly lower (t -test $p = 9.46 \times 10^{-5}$).

Comparison of blood collection protocols. To investigate how cfDNA yield and LMW fractions were affected by blood collection tubes and protocols, we collected 3 blood samples each from 23 healthy volunteers (12 males and 11 females): one EthyleneDiamineTetraacetic Acid (EDTA) tube processed within 1 hour and two Cell-free DNA Blood Collection Tubes (BCT) stored at ambient temperature for 24 hours and 72 hours prior to processing (labeled here as BCT 24 hr and BCT 72 hr respectively). We processed all samples identically and extracted cfDNA using QIAamp Circulating Nucleic Acid kit (QIAGEN). We measured cfDNA yield and fragment size using ddPCR. Mean LMW GEs/mL plasma for EDTA, BCT 24 hr, and BCT 72 hr were 1,925, 1,591, and 1,514 respectively with no significant difference between collection protocols (ANOVA $p = 0.439$, Fig. 4a and Supplemental Table 5). LMW fractions for EDTA, BCT 24 hr, and BCT 72 hr were 87%, 88%, and 90% respectively with no significant difference (ANOVA $p = 0.083$, Fig. 4b).

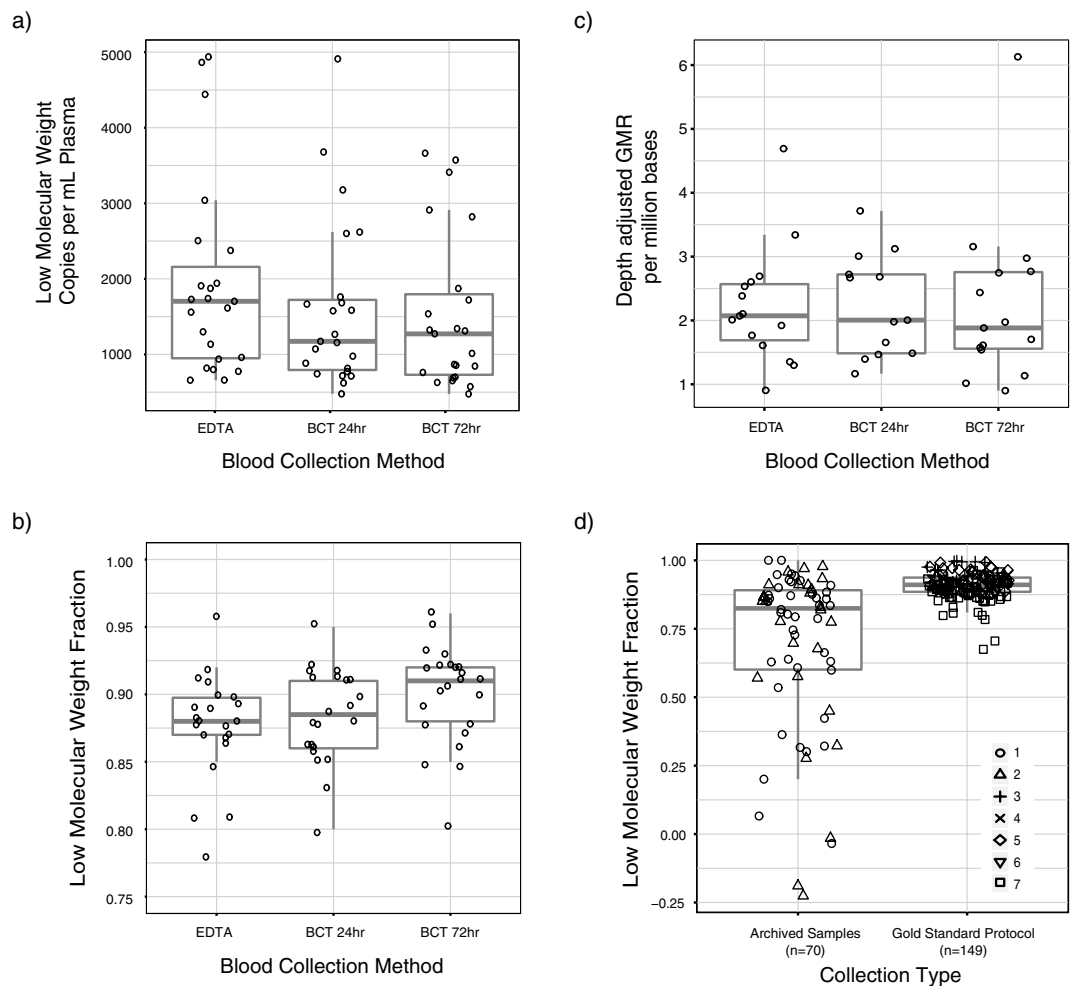


Figure 4. (a,b,c) Evaluation of blood collection protocols for cfDNA analysis using ddPCR and digital targeted sequencing. (a,b) Comparison of cfDNA yield (in LMW fragments/mL of plasma) and LMW fraction across 3 blood collection methods. Outliers at 0.67 LMW fraction for EDTA and at 0.71 LMW fraction for BCT 24 hr are not shown in (b) to enhance scaling. Paired samples from healthy volunteers were collected for this analysis. Comparison between EDTA, BCT 24 hr samples and BCT 72 hr samples showed no significant difference for yield or LMW fraction (ANOVA p-values > 0.05). Concentration of LMW fragments in DNA samples was calculated as the difference between average short and long GEs (as shown in Fig. 1). To calculate concentration in input plasma samples, the LMW fragment concentration in DNA samples was multiplied by the elution volume used at the time of plasma DNA extraction and divided by the volume of plasma used. LMW fraction was calculated as LMW fragment concentration (difference between average short and long GEs) as a fraction of average short GEs. (c) Comparison of depth-adjusted GMR observed across collection protocols. Pairwise comparisons between EDTA and BCT 24 hr samples ($n = 12$ pairs) and between EDTA and BCT 72 hr samples ($n = 13$) showed no significant difference between collection protocols (paired t-test $p > 0.05$). (d) Comparison of LMW fraction between archived retrospective samples and samples processed using gold standard protocols for ctDNA analysis, showing significant difference between the two groups ($n = 219$ plasma samples, t-test $p = 2.302 \times 10^{-7}$). Symbols indicate cohort numbers with details in Supplemental Tables 6 and 7. Samples in the gold standard cohorts were collected in EDTA tubes, spun for 10 mins at 820 g, aliquoted to 1 mL, spun again for 10 mins at maximum speed (16,000–20,000 g) and stored at -80°C , within 1–3 hours. Details of sample processing for all cohorts are described in Supplemental Table 6. For 4 archived samples, LMW fraction was measured as a negative number. Potential drivers of a negative LMW fraction include (1) sampling variation when input DNA is nearly 100% intact but concentration is low; (2) copy number variations affecting one or more loci in a very high tumor fraction plasma sample and 3) underestimated short GEs due to overloading, when input DNA is nearly 100% intact and concentration is very high. Our assay targets 5 short amplicons and 4 long amplicons. Assuming intact DNA, when a ddPCR reaction is overloaded, the assumption of single droplet occupancy will be violated earlier for short amplicons and despite Poisson correction for droplet loading, we are likely to underestimate short GEs. For 2 of 4 samples with negative LMW fraction (-18.9 and -22.5%), we measured the highest long GEs of all included samples, suggesting the input DNA was nearly 100% intact and we underestimated short GEs in these measurements due to overloading. In the third and fourth sample (LMW fraction -3.4 and -1.5%), we measured a few additional copies of the genome using long amplicons compared to short (314 long vs. 309 short GEs and 490 long vs. 474 short GEs), suggesting sampling noise and nearly 100% intact DNA.

To assess whether cell-stabilizing preservative would affect background noise in cfDNA sequencing, we prepared targeted sequencing libraries using a molecular tagging approach that can help distinguish non-reference alleles arising in the original template molecules from errors introduced during PCR amplification. We sequenced 43 samples including all 3 pairs from 12 individuals and 7 additional samples. We generated an average of 7.64 million read pairs per sample and achieved mean unique coverage in the target region of 37.0 read families (with an average 3.92 members/read family). To measure background noise, we calculated global nucleotide mismatch rate (GMR) as the sum of the number of read families with non-reference alleles divided by the sum of unique coverage across all targeted loci (additional details in Methods). GMR per million bases was 37.8 ± 12.2 , 30.8 ± 9.11 and 30.8 ± 7.77 for EDTA, BCT 24 hr and BCT 72 hr samples respectively (mean \pm standard deviation). GMR between paired samples from the same individuals was highly correlated across tube types (Pearson $r = 0.652$, 0.647 and 0.758 , $p = 0.022$, 0.017 and 0.003 for the three pairwise comparisons, Supplemental Figure 5). This suggests that biological noise (*in vivo*) was a much larger contributor to measured GMR instead of noise introduced during sample processing or analysis. Since depth of coverage would determine our ability to measure low-abundance noise, we adjusted GMR by unique depth of coverage and found no significant difference between EDTA and BCT 24 hr as well as EDTA and BCT 72 hr samples (paired t-test $p = 0.998$, $n = 12$ pairs and $p = 0.451$, $n = 13$ pairs respectively, Fig. 4c).

Evaluation of cfDNA fragment size in clinical samples. To evaluate the extent to which background DNA from peripheral cell lysis affects cfDNA analysis in archived retrospective samples, we evaluated a cohort of 219 clinical samples collected across 7 cohorts and multiple collection sites (Supplemental Table 6). Using the ddPCR assay, we found that LMW fractions were significantly lower in archived samples (cohorts 1 and 2, $n = 70$ samples, median LMW fraction: 82.5%) compared to plasma samples collected prospectively for cfDNA analysis and immediately processed using current gold standard protocols (cohorts 3–7, $n = 149$ samples, median LMW fraction: 91.1%, t-test $p = 2.302 \times 10^{-7}$, Fig. 4d and Supplemental Tables 5 and 7).

Discussion

Variation in pre-analytical processing of plasma samples can affect results of cfDNA analysis¹². Circulating cell-free DNA is predominantly fragmented and delays between venipuncture and isolation of plasma can lead to higher background of intact DNA contributed by lysis of peripheral blood cells¹³. This affects PCR and tagmentation-based sequencing methods by diluting the measured mutation fractions and it affects ligation-based sequencing methods by lowering effective template available for analysis. We have developed a multiplexed droplet digital PCR approach to reliably assess amplifiable quantities of cfDNA and estimate the contribution of high molecular weight background DNA in a single step. As an upfront sample quality assessment assay, this approach can help optimize input quantities to achieve reproducible performance in sequencing experiments. The assay design targets 9 different regions in the genome, lowering minimum input DNA quantity needed for quality assessment. qPCR or digital PCR assays that target 1–2 loci can be biased by locus-specific amplification bias or by somatic copy number changes in plasma samples from advanced cancer patients¹⁷. Instead, we rely on average readouts across multiple targets to achieve high precision from limited quantities of cfDNA and to accommodate the wide range of total cfDNA concentrations found in patients with cancer (particularly when implemented in ddPCR with millions of partitions). Although widespread aneuploidy in the tumor can still affect our approach, targeting multiple loci limits the impact of any single copy number alteration on the final quantification. Nevertheless, a PCR based approach to quantify cfDNA may under- or over-estimate total cfDNA levels in plasma samples from a fraction of patients with advanced, widely aneuploid cancers and very high fractions of tumor-derived DNA in plasma.

Several new solutions to streamline cfDNA extraction have been introduced recently including magnetic-bead based approaches but published reports have not compared these with existing methods^{17–20}. To provide an update and compare cfDNA extraction performance using a robust approach, we evaluated seven commercially available kits marketed for cfDNA extraction and found that QIAamp Circulating Nucleic Acid kit provided the highest cfDNA yield and low molecular weight fractions. Newer methods that use magnetic beads for DNA extraction may be more automatable and in our results, the MagMAX Cell-free DNA Isolation kit provided the highest yield and low molecular weight fractions amongst such workflows.

To overcome the need for rapid processing of plasma samples, special blood collection tubes are available that include a preservative to prevent lysis of peripheral blood cells for up to several days at room temperature²¹. Current applications for cfDNA analysis in prenatal diagnostics rely on relative representation of genomic regions but in patients with cancer, there is need for detection of mutations at very low fractional abundance and preservative induced noise could lead to false positives. In paired samples from healthy volunteers, we found no evidence that cfDNA yield or fragment size was significantly different between EDTA tubes processed within 1 hour of collection and BCT tubes stored at ambient temperature and processed 72 hours after collection. These results are in agreement with published observations^{22–25}. In addition, we also extensively explored whether preservative in BCT tubes induced any pre-analytical noise using digital targeted sequencing. To ensure that we could measure pre-analytical noise separately from any errors introduced during library preparation, we used a molecularly tagged sequencing strategy. We found no evidence that global mutation rate (adjusted for depth of sequencing) is any different in blood stored in BCT tubes at ambient temperature for up to 72 hours after collection as compared to samples collected in EDTA tubes and processed within 1 hour. Interestingly, we observed that GMR was highly correlated between independent replicates from the same individual across blood processing protocols, even after thorough filtering for common and private germline SNPs. This suggests that once sequencing errors are filtered out, biological noise introduced *in vivo* is the predominant contributor to GMR instead of pre-analytical errors introduced *in vitro*. Such biological noise may arise from non-specific somatic mutations (potentially originating in circulating blood cells) or extracellular damage to cfDNA during circulation. Although we cannot distinguish

between these mechanisms based on our results, this observation warrants further study particularly as the field investigates circulating tumor DNA analysis for early detection of cancer.

There are multiple limitations of this study that must be acknowledged. Library preparation kits differ in their efficiency and performance and can be affected by multiple factors such as adapter composition, input DNA concentration and ligation time. While the absolute measurements of library yield and diversity may not be valid for other library preparation methods, accurate quantification and size assessment of input cfDNA will still be relevant. Similarly, several factors can affect DNA extraction yield including input plasma volumes and elution volumes. When comparing cfDNA extraction methods, we minimized biological background by testing 70 replicates of 1 mL each from a single pooled plasma sample. Extraction performance of the tested kits may differ from our results if a different volume of plasma is used. Moreover, our analysis is limited to 7 commercially available cfDNA extraction solutions including 3 kits that use spin columns and 4 kits that use magnetic beads. There are several additional solutions for cfDNA extraction available and our results will not be directly relevant for any solutions not tested in this study. For comparison of blood collection and processing protocols, we performed paired analysis of samples and found no appreciable differences in background noise between EDTA and BCT tubes. Our effective sample size for the sequencing-based comparison is limited to 13 pairs and that could limit power to detect subtle differences in pre-analytical error rates but there are no indications of even a trend towards a difference in depth-adjusted GMR between collection protocols. In addition, comparison of blood processing protocols was performed on samples obtained from healthy volunteers and we cannot directly comment on whether tumor-specific mutant DNA will behave similarly.

In summary, we have developed a droplet digital PCR based approach to assess quantity and quality of plasma DNA samples to improve performance of downstream sequencing assays. We presented comparison of several methods for cfDNA extraction and blood collection for cfDNA and their potential effects on downstream analysis. We now routinely use this assay for quality assessment of all plasma samples processed and analyzed for ctDNA studies in our lab. We find significant differences in quality between archived samples and prospectively collected plasma samples, processed rapidly for ctDNA analysis, highlighting the importance and need for appropriate pre-analytical processing of samples. Since archived samples from clinical trials are often accompanied by long-term follow-up and clinical annotation, their use can be critical to evaluate clinical utility of ctDNA analysis in cancer patients. The ddPCR approach we describe here will be useful to assess quality of archived samples prior to analysis and to inform interpretation of downstream results. Our findings can benefit the design of future studies and clinical trials by helping minimize the contribution of pre-analytical variability in circulating tumor DNA analysis.

Methods

Droplet Digital PCR to assess quantity and fragment size. We designed a multiplexed ddPCR assay targeting 9 single copy genomic loci¹⁶. We included 5 short PCR amplicons with mean product size of 71 bp (range 67–75 bp) and corresponding probes labeled with FAM as well as 4 long PCR amplicons with mean product size of 471 bp (range 439–522 bp) and corresponding probes labeled with TET (Fig. 1 and Supplemental Table 1). We used PrimerQuest (Integrated DNA Technologies) to design these assays, evaluated them to avoid known polymorphic loci (snapshots from UCSC genome browser indicate common SNPs relative to primer and probe loci in Supplemental Figure 6). We used *in silico* PCR to confirm each amplicon yielded a single product and no cross products when used in multiplex, using a command-line version of UCSC *In Silico* PCR to evaluate primers in batch.

We prepared digital PCR reactions at 50 μ L volume using 25 μ L of 2 \times KAPA PROBE FAST Master Mix (Kapa Biosystems), 2 μ L of 5 mM dNTP Mix (Kapa), 2 μ L of 25 \times Droplet Stabilizer (RainDance Technologies), 9 μ L of 100 μ M primer mix (pooled equimolarly), 1.68 μ L of 20 μ M each probe (IDT), 0.25 μ L molecular biology grade water and 2–10 μ L of input DNA. We generated droplets using RainDrop Digital PCR Source Instrument (RainDance), performed thermocycling using DNA Engine Tetrad 2 (Bio-Rad Laboratories) with the following parameters: 1 cycle of 3 min at 95 $^{\circ}$ C, 50 cycles of 15 sec at 95 $^{\circ}$ C and 1 min at 60 $^{\circ}$ C with a 0.5 $^{\circ}$ C/sec ramp from 95 $^{\circ}$ C to 60 $^{\circ}$ C, 1 cycle of 98 $^{\circ}$ C for 10 min and hold at 4 $^{\circ}$ C forever. We measured droplet fluorescence using RainDrop Digital PCR Sense Instrument (RainDance) and analyzed results using accompanying software.

Identification of positive droplets requires setting fluorescence thresholds (gates) for each ddPCR assay (Fig. 1). We compared results across intact genomic DNA and no template controls to identify thresholds for this assay. We calculated fractional loss of volume (dead volume) as the difference between measured number of intact droplets of expected size (5 pL) and number of expected droplets (10 million droplets for 50 μ L reactions). Any reactions with > 50% loss of volume were excluded from further analysis.

Using uniform gates across all samples, we measured two populations of droplets: FAM-labeled droplets with short amplicons and TET-labeled droplets with long amplicons. We calculated short and long haploid Genome Equivalents (GEs) by dividing short and long droplet counts by number of targeted assays (5 and 4 respectively). We further calculated GE concentration by accounting for input DNA volume. We calculated LMW fragment concentration by taking the difference between long and short GEs (Fig. 1). We calculated LMW fragment concentration in plasma as the product between LMW fragment concentration in the DNA sample and elution volume divided by plasma volume used for DNA extraction. We calculated LMW fraction as the LMW fragment concentration in DNA sample expressed a fraction of short GEs.

Evaluation of assay performance. For any given PCR reaction, yield is affected by amplicon size and template fragment size. To evaluate whether our ddPCR assay performed as expected, we analyzed known quantities of sheared DNA fragments with predetermined size and compared the results with expected theoretical yields. To generate experimental data, we analyzed 4 aliquots of 0.6 ng/ μ L human genomic DNA (Sigma Aldrich), sheared by sonication to achieve fragment sizes of 150 bp, 300 bp, 500 bp and 1,000 bp. To estimate theoretical yield, we

performed simulations of DNA fragmentation as described previously²⁶. Assuming a DNA molecule spanning 2,500 bp on either side of the average amplicon size for each set (5,071 bp for short amplicons and 5,471 bp for long amplicons), we generated break points by sampling from an exponential distribution with a rate representing the corresponding fragment size (150, 300, 500 or 1,000 bp). We determined that a molecule will be “missed” by an amplicon if a DNA break fell within the amplicon region (bound by 5' ends of the two primers). We sampled 50,000 molecules to determine overall frequency of missed molecules for each combination of amplicon size and fragment size.

Comparison of cfDNA extraction kits. We obtained 250 mL of a control pooled plasma sample collected with K2 EDTA additive from BioreclamationIVT. Upon receipt, the sample was thawed and stored in 1 mL aliquots at -80°C until further analysis. We compared 7 different extraction kits marketed for cfDNA extraction including 3 spin column-based methods and 4 magnetic beads-based methods (labeled A-G, see Supplemental Table 3). Manufacturer recommended protocols for plasma DNA extraction were followed. Prior to each extraction, plasma aliquots were centrifuged at 14,000 g for 10 minutes to remove any cellular debris.

Comparison of blood collection protocols. To compare cfDNA yield, fragment size and sequencing noise across blood collection protocols, we collected plasma samples from healthy volunteers. We collected 8–10 mL blood in K2 EDTA BD Vacutainer tubes and two Cell-Free DNA BCT (Streck) from each volunteer²¹. EDTA tube was processed within 1 hour of collection. cfDNA BCT were stored at ambient temperature and processed 24 and 72 hours after collection. Samples were centrifuged at 820 g for 10 min at room temperature. 1 mL aliquots of plasma were further centrifuged at 16,000 g for 10 mins to pellet any remaining cellular debris. The supernatant was stored at -80°C until DNA extraction. DNA was extracted using the QIAamp Circulating Nucleic Acid kit (QIAGEN). cfDNA yield and fragment size were evaluated using ddPCR. Baseline sequencing noise was evaluated using digital sequencing, targeting a panel of recurrent cancer genes.

Clinical samples. Healthy volunteer and clinical plasma samples included in comparison of immediately processed and archived samples were collected after obtaining informed consent under multiple independent clinical protocols, all approved by Western IRB (protocol number 20142638). All experiments were performed in accordance with relevant guidelines and regulations. Samples from 7 independent clinical cohorts were included in this analysis, including patients diagnosed with melanoma, cholangiocarcinoma and rectal cancer as well as healthy volunteers. Sample processing conditions and number of samples from each cohort are described in Supplemental Table 6. 7 samples, all from the same ddPCR chip, were excluded from this analysis due to $> 50\%$ loss of volume during ddPCR. Median dead volume across remaining samples was 10.4% ($n = 219$ samples).

Sequencing library preparation. For assessment of sequencing performance guided by ddPCR results, we quantified cfDNA from control plasma samples (commercially obtained) using ddPCR and prepared whole genome sequencing libraries using ThruPLEX DNA-Seq (Rubicon Genomics), as per manufacturer's instructions. We compared performance across 1, 2 and 5 ng amounts of input DNA and concentrated samples to achieve 10 μL starting volume if needed (using vacuum concentration). We assigned sample specific barcodes to each library, quantified them using qPCR and pooled them at equimolar concentrations for target enrichment. We performed exome enrichment using NimbleGen SeqCap EZ Human Exome v3 kit (Roche), as per manufacturer's instructions except the use of xGen Universal Blocking Oligos – TS HT-i5 and TS HT-i7 (IDT). We quantified all enriched exome libraries using qPCR and pooled at equimolar concentrations for sequencing. We performed sequencing on MiSeq (Illumina) to generate 75 bp paired-end reads and a 6 bp barcode read.

For comparison of background noise between blood collection tubes, we prepared whole genome sequencing libraries from 1 ng cfDNA from volunteer plasma samples using ThruPLEX Tag-seq (Rubicon). This kit introduces a 6 bp random molecular tag on both sides of DNA fragments, making it possible to distinguish any non-reference alleles (true mutations or pre-analytical noise) in the original template molecule from PCR noise introduced during library preparation. We quantified the libraries and pooled them for target capture using xGen[®] Pan-Cancer Panel (IDT), following manufacturer's instructions.

Sequencing data analysis. We demultiplexed sequencing data based on sample-specific barcodes and converted to fastq files using Picard tools v2.2.1, allowing 1 bp mismatch and requiring minimum base quality of 30. We aligned sequencing reads to the human genome hg19 using bwa mem v0.6.2²⁷. We sorted and indexed bam files using samtools v1.3.1²⁸ and calculated library diversity using Picard tools.

For data comparing background noise across blood collection tubes, we added a barcode (BC) tag comprised of the two paired 6 bp unique molecular identifiers (UMIs) to each aligned read. We parsed these BAM files using a custom R script to identify UMI families and assign read groups as follows: For each set of reads that started and ended at the same genomic positions, we sorted UMI pairs by the number of exact duplicates observed. We used the most frequent UMI pair in this set to seed the first read family. For the remaining reads, if either of the 2 UMIs in a pair were within a Hamming distance of 1 from the corresponding seed UMI, we assigned them to the same read family. For any UMIs not assigned in the first cycle, we repeated this process starting with the next most frequent UMI pair until all reads had been assigned read families. We grouped reads from the same family by adding RG tags to the BAM files. To facilitate computational processing, we assumed fragment sizes in our libraries would not exceed 1,000 bp.

Once all reads were assigned RG tags, we generated pileups per read-family using samtools mpileup. Each read family with ≥ 3 members was included in further analysis. We required $\geq 80\%$ of reads supporting a non-reference allele to call a variant. All variants overlapping with dbSNP v147 were removed. To avoid any private SNPs, we filtered out positions covered by < 10 read families or total non-reference allele fraction $\geq 20\%$. We calculated global nucleotide mismatch rate (GMR) as the sum of the number of read families with non-reference

alleles divided by the sum of unique coverage across all targeted loci. To account for variability in depth of coverage between samples, we adjusted GMR for average unique coverage in each sample.

Data Availability Statement. The datasets generated during and analyzed during the current study are available from the corresponding author on reasonable request.

References

- Bianchi, D. W. *et al.* DNA sequencing versus standard prenatal aneuploidy screening. *The New England journal of medicine* **370**, 799–808, <https://doi.org/10.1056/NEJMoa1311037> (2014).
- De Vlaminck, I. *et al.* Circulating cell-free DNA enables noninvasive diagnosis of heart transplant rejection. *Science translational medicine* **6**, 241ra277, <https://doi.org/10.1126/scitranslmed.3007803> (2014).
- Haber, D. A. & Velculescu, V. E. Blood-based analyses of cancer: circulating tumor cells and circulating tumor DNA. *Cancer Discov* **4**, 650–661, <https://doi.org/10.1158/2159-8290.CD-13-1014> (2014).
- Lo, Y. M. & Chiu, R. W. Genomic analysis of fetal nucleic acids in maternal blood. *Annual review of genomics and human genetics* **13**, 285–306, <https://doi.org/10.1146/annurev-genom-090711-163806> (2012).
- Bettgowda, C. *et al.* Detection of circulating tumor DNA in early- and late-stage human malignancies. *Science translational medicine* **6**, 224ra224, <https://doi.org/10.1126/scitranslmed.3007094> (2014).
- Dawson, S. J. *et al.* Analysis of circulating tumor DNA to monitor metastatic breast cancer. *The New England journal of medicine* **368**, 1199–1209, <https://doi.org/10.1056/NEJMoa1213261> (2013).
- Forshew, T. *et al.* Noninvasive identification and monitoring of cancer mutations by targeted deep sequencing of plasma DNA. *Science translational medicine* **4**, 136ra168, <https://doi.org/10.1126/scitranslmed.3003726> (2012).
- Newman, A. M. *et al.* Integrated digital error suppression for improved detection of circulating tumor DNA. *Nat Biotechnol* **34**, 547–555, <https://doi.org/10.1038/nbt.3520> (2016).
- Wan, J. C. *et al.* Liquid biopsies come of age: towards implementation of circulating tumour DNA. *Nat Rev Cancer* **17**, 223–238, <https://doi.org/10.1038/nrc.2017.7> (2017).
- Wong, D. *et al.* Optimizing blood collection, transport and storage conditions for cell free DNA increases access to prenatal testing. *Clinical biochemistry* **46**, 1099–1104, <https://doi.org/10.1016/j.clinbiochem.2013.04.023> (2013).
- Jiang, P. *et al.* Lengthening and shortening of plasma DNA in hepatocellular carcinoma patients. *Proc Natl Acad Sci USA* **112**, E1317–1325, <https://doi.org/10.1073/pnas.1500076112> (2015).
- Sherwood, J. L. *et al.* Optimised Pre-Analytical Methods Improve KRAS Mutation Detection in Circulating Tumour DNA (ctDNA) from Patients with Non-Small Cell Lung Cancer (NSCLC). *PLoS One* **11**, e0150197, <https://doi.org/10.1371/journal.pone.0150197> (2016).
- Chiu, R. W. *et al.* Effects of blood-processing protocols on fetal and total DNA quantification in maternal plasma. *Clinical chemistry* **47**, 1607–1613 (2001).
- Jung, M., Klotzek, S., Lewandowski, M., Fleischhacker, M. & Jung, K. Changes in concentration of DNA in serum and plasma during storage of blood samples. *Clinical chemistry* **49**, 1028–1029 (2003).
- Chan, K. C., Yeung, S. W., Lui, W. B., Rainer, T. H. & Lo, Y. M. Effects of preanalytical factors on the molecular size of cell-free DNA in blood. *Clinical chemistry* **51**, 781–784, <https://doi.org/10.1373/clinchem.2004.046219> (2005).
- Eisenberg, E. & Levanon, E. Y. Human housekeeping genes, revisited. *Trends Genet* **29**, 569–574, <https://doi.org/10.1016/j.tig.2013.05.010> (2013).
- Devonshire, A. S. *et al.* Towards standardisation of cell-free DNA measurement in plasma: controls for extraction efficiency, fragment size bias and quantification. *Anal Bioanal Chem* **406**, 6499–6512, <https://doi.org/10.1007/s00216-014-7835-3> (2014).
- Mauger, F., Dulary, C., Daviaud, C., Deleuze, J. F. & Tost, J. Comprehensive evaluation of methods to isolate, quantify, and characterize circulating cell-free DNA from small volumes of plasma. *Anal Bioanal Chem* **407**, 6873–6878, <https://doi.org/10.1007/s00216-015-8846-4> (2015).
- Repiska, G., Sedlackova, T., Szemes, T., Celec, P. & Minarik, G. Selection of the optimal manual method of cell free fetal DNA isolation from maternal plasma. *Clin Chem Lab Med* **51**, 1185–1189, <https://doi.org/10.1515/cclm-2012-0418> (2013).
- Fleischhacker, M. *et al.* Methods for isolation of cell-free plasma DNA strongly affect DNA yield. *Clin Chim Acta* **412**, 2085–2088, <https://doi.org/10.1016/j.cca.2011.07.011> (2011).
- Fernando, M. R. *et al.* A new methodology to preserve the original proportion and integrity of cell-free fetal DNA in maternal plasma during sample processing and storage. *Prenat Diagn* **30**, 418–424, <https://doi.org/10.1002/pd.2484> (2010).
- Kang, Q. *et al.* Comparative analysis of circulating tumor DNA stability in K3EDTA, Streck, and CellSave blood collection tubes. *Clinical biochemistry* **49**, 1354–1360, <https://doi.org/10.1016/j.clinbiochem.2016.03.012> (2016).
- Toro, P. V. *et al.* Comparison of cell stabilizing blood collection tubes for circulating plasma tumor DNA. *Clinical biochemistry* **48**, 993–998, <https://doi.org/10.1016/j.clinbiochem.2015.07.097> (2015).
- Parpart-Li, S. *et al.* The effect of preservative and temperature on the analysis of circulating tumor DNA. *Clin Cancer Res*, <https://doi.org/10.1158/1078-0432.CCR-16-1691> (2016).
- El Messaoudi, S., Rolet, F., Mouliere, F. & Thierry, A. R. Circulating cell free DNA: Preanalytical considerations. *Clin Chim Acta* **424**, 222–230, <https://doi.org/10.1016/j.cca.2013.05.022> (2013).
- Xie, J., Crooke, P. S., McKinney, B. A., Soltman, J. & Brandt, S. J. A computational model of quantitative chromatin immunoprecipitation (ChIP) analysis. *Cancer Inform* **6**, 138–146 (2008).
- Li, H. Aligning sequence reads, clone sequences and assembly contigs with BWA-MEM. *arXiv preprint arXiv:1303.3997* (2013).
- Li, H. *et al.* The Sequence Alignment/Map format and SAMtools. *Bioinformatics* **25**, 2078–2079, <https://doi.org/10.1093/bioinformatics/btp352> (2009).

Acknowledgements

We gratefully acknowledge support for this study through a Bisgrove Scholars Award from Science Foundation Arizona. We also acknowledge support from The V Foundation, Stand Up To Cancer, Ben and Catherine Ivy Foundation and Desert Mountain CARE. We would like to thank Stephanie Althoff and Stephanie Buchholtz at TGen, volunteers and patients who participated in this study.

Author Contributions

M.M. and T.C. designed the study. T.C., H.M. and W.S.L. performed the experiments. M.J.B., S.S., S.G., N.L.T., H.D.D., M.E.B., A.B., A.S., A.R., J.M.T. and P.M.L. designed and performed clinical studies and performed clinical interpretation. H.M. and M.M. performed data analysis and wrote the manuscript. All authors reviewed the manuscript.

Additional Information

Supplementary information accompanies this paper at <https://doi.org/10.1038/s41598-018-25810-0>.

Competing Interests: M.M., H.M. and T.C. are inventors or contributors on patent applications describing methods for circulating tumor DNA analysis including methods and results described in this manuscript. All other authors declare no potential conflict of interest.

Publisher's note: Springer Nature remains neutral with regard to jurisdictional claims in published maps and institutional affiliations.



Open Access This article is licensed under a Creative Commons Attribution 4.0 International License, which permits use, sharing, adaptation, distribution and reproduction in any medium or format, as long as you give appropriate credit to the original author(s) and the source, provide a link to the Creative Commons license, and indicate if changes were made. The images or other third party material in this article are included in the article's Creative Commons license, unless indicated otherwise in a credit line to the material. If material is not included in the article's Creative Commons license and your intended use is not permitted by statutory regulation or exceeds the permitted use, you will need to obtain permission directly from the copyright holder. To view a copy of this license, visit <http://creativecommons.org/licenses/by/4.0/>.

© The Author(s) 2018